

An Adaptive Chimney Stack for Noise Control

M. R. F. Kidner and B. S. Cazzolato

(1) Active Noise and Vibration Control Group, Dept. Mechanical Engineering University of Adelaide SA 5006.

ABSTRACT

Radiation of noise from exhaust stacks is a significant source of community disturbance. In this paper an exhaust stack with an adaptive length is proposed. The effective length of the stack is changed by altering the level of water in a sump at the base of the stack, this level is controlled as a function of the radiated noise from the top of the stack. The system is modelled as a pipe with an adaptive side branch. A gradient descent algorithm is used to minimise the radiated sound. The response to a step change in frequency and a chirp signal is shown. A simple heuristic controller is compared to the performance obtained with the gradient descent algorithm and is shown to be acceptable and computationally simpler.

INTRODUCTION

One of the significant sources of community disturbance is noise radiation from exhaust stacks, this noise is tonal in nature and so is heavily weighted in evaluations of annoyance (Bies 1992). Retrofitting noise mitigation measures to industrial plants is very expensive and minimisation of downtime is an important factor in keeping costs low. The adaptive noise control approach suggested here would be applicable to many exhaust stacks because of the controller simplicity, an installation that does not interfere substantially with the exhaust stack operation and the small number of electro-acoustic transducers required. Side branches in exhaust systems have been used to reduce noise, (Kinsler 1999), but also have been identified as noise sources (Selemat 1996), the noise created being a function of sidebranch length and cross sectional area. An adaptive passive control system for noise in ducts has been proposed by Kostek (Kostek 1999) and has been used effectively to control noise. In this work the stack length is changed using an extendable section. This approach can achieve a larger range of operation frequencies but is expensive as the entire stack needs to be amended. The adaptive stack proposed here can be modeled as an open-ended pipe with a variable length side branch attached, see Figure (1).

THEORETICAL PERFORMANCE OF THE CONTROLLER

In this section we develop a model of the plant and design a controller. First, the radiation from a pipe as a function of its length is determined, from this an appropriate controller is designed.

Radiation from an open pipe with a side branch

The sound power radiated from a pipe is a function of its impedance, (Beranek 1992) and the acoustic impedance of the surroundings. However it can be hard to predict for very resonant systems, (Davis 2004), The change in the radiated sound power as a function of the drive frequency, normalised to the wavelength is shown in Figure (2). It can be seen that there is a strong dependence on the length of the side branch. However it is not a linear relationship between side branch length and radiated sound power.

The model of the exhaust system was developed using transfer matrixes after Beranek & Ver.

The transfer matrix, that relates pressures and mass flow rates for a section of pipe can be written as

$$T_{pipe} = \begin{bmatrix} T_{11} & T_{12} \\ T_{21} & T_{22} \end{bmatrix} = e^{-jk_c M l} \begin{bmatrix} \cos(k_c l) & jY_0 \sin(k_c l) \\ \frac{j \sin(k_c l)}{Y_0} & \cos(k_c l) \end{bmatrix} \quad (1)$$

where k , c , and l are the wavenumber, sound speed and length of the pipe section respectively. The Mach number of the flow in the pipe is indicated by M . Y_0 is defined by c/S_0 , the ratio of sound speed to the cross sectional area of the pipe. So that

$$\begin{bmatrix} p_2 \\ \rho S u_2 \end{bmatrix} = \mathbf{T} \begin{bmatrix} p_1 \\ \rho S u_1 \end{bmatrix} \quad (2)$$

where p is the pressure and u the particle velocity. The density of the fluid and cross sectional area of the pipe is indicated by ρ and S respectively.

For a side branch resonator the transfer impedance is given by Equation (3)

$$T_r = \begin{bmatrix} 1 & 0 \\ \frac{1}{Z_t + Z_c} & 1 \end{bmatrix} \quad (3)$$

where Z_t , the throat impedance and Z_c , the cavity impedance of a side branch tube, are defined as

$$Z_t = \frac{ck^2}{\pi} + j \frac{ck(l_c + 1.7r_0)}{S_0} \quad Z_c = -j \frac{c}{S_c} \cot(kl_c) \quad (4)$$

where r and S_0 are the radius of the branch and the cross sectional area of the side branch respectively. The lengths of the throat and the length of the side branch itself are indicated by l_t and l_c .

From these equations the pressure radiated from the end of the pipe, shown in Figure (1) can be calculated by multiplication of the transfer matrices for each section.

$$\mathbf{P}_3 = \mathbf{T}_3 \mathbf{T}_2 \mathbf{T}_1 P_1 \quad (5)$$

The overall transfer matrix for the exhaust stack can be written as

$$\mathbf{T} = \mathbf{T}_3 \mathbf{T}_2 \mathbf{T}_1 \quad (6)$$

The pressure at the radiating end can be written as

$$\begin{aligned} P_3 &= \mathbf{T}_{(1,1)} p_1 + \mathbf{T}_{(1,2)} \rho S u_1 \\ &= \left(\mathbf{T}_{(1,1)} + \frac{S}{c} \mathbf{T}_{(1,2)} \right) p_1 \end{aligned} \quad (7)$$

the velocity at the radiating end can be written as

$$\begin{aligned} u_3 &= \frac{1}{\rho S} \mathbf{T}_{(2,1)} p_1 + \mathbf{T}_{(2,2)} \rho S u_1 \\ &= \frac{1}{\rho S} \left(\mathbf{T}_{(2,1)} + \frac{S}{c} \mathbf{T}_{(2,2)} \right) p_1 \end{aligned} \quad (8)$$

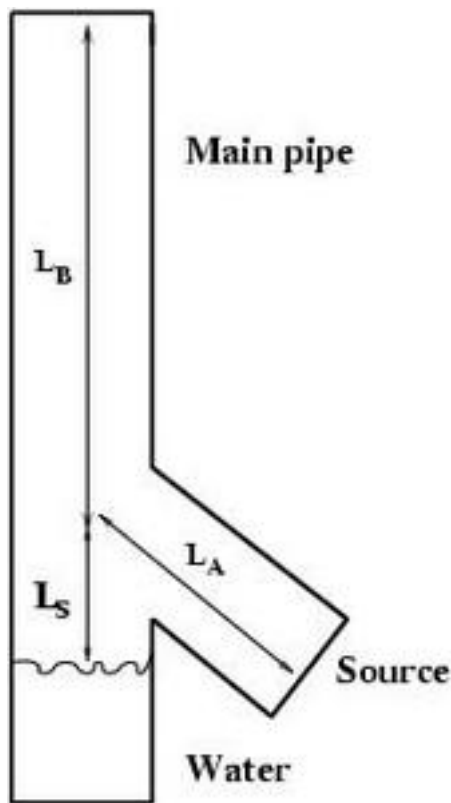


Figure 1 Simplification of exhaust stack with side branch.

The stack radiates into free space and so the correct radiation impedance should be included. At the radiating end of the stack the following relationship must hold:

$$p_{rad} = Z_r U_{rad} \quad (9)$$

where, $U_{rad} = S u_3$, the volume velocity at the radiating end, and $p_{rad} + p_3 = 0$.

Therefore the radiating pressure can be written as

$$p_{rad} = Z_r S u_3 = Z_{rad} \left(\mathbf{T}_{(2,1)} + \frac{\rho S}{c} \mathbf{T}_{(2,2)} \right) p_1 \quad (11)$$

The expression in (11) allows the radiated pressure to be calculated, this is used to simulate the behaviour of the control system. However to evaluate the system the standard calculation for the insertion loss is used. The insertion loss is calculated using equation (12).

$$IL = 20 \log_{10} \left| \frac{\mathbf{T}_{(1,1)} Z_t + \mathbf{T}_{(1,2)} + \mathbf{T}_{(2,1)} Z_t Z_s + \mathbf{T}_{(2,2)} Z_s}{Z_t + Z_s} \right|$$

where \mathbf{T} is the transfer matrix of the system, Z_s and Z_t are the source and termination impedances respectively.

Possible frequency range of control

From Figure (3) it can be seen that the insertion loss of a tone in the frequency range 100-200Hz could be varied by up to 40dB, depending on the length of the side branch. The peaks in insertion loss are sharp and so an accurate controller is required.

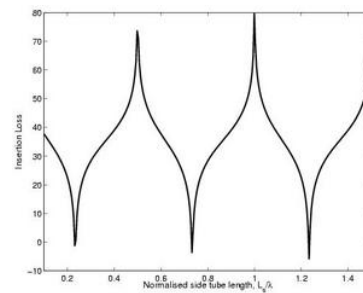


Figure 2 Variation in insertion loss as a function of the length of the side pipe, normalised to wavelength.

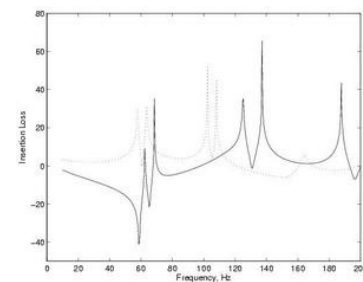


Figure 3 Insertion loss of the side branch at minimum (solid line) and maximum (dotted line) length.

CONTROL SYSTEMS FOR THE ADAPTIVE EXHAUST STACK

We will consider two control algorithms, one gradient based and the other rule based. The gradient descent algorithm should give results that indicate a best case scenario, however it is not the most practical controller because the gradient calculation requires additional alterations of the side branch length. This may result in undesirable fluctuations in the radiated sound power as the system converges. The rule based method is far simpler, but may have slower convergence rate and a higher steady state error. It is also likely to require more tuning to obtain good performance. These factors will be discussed in the following sections.

A general control flow diagram is shown in Figure (4), in this system the control action is a function of the error magnitude and the gradient of the error with respect to the length of the side branch. The gains G_p and G_d control the contribution of the proportional and derivative part. The system H is the water pump, and is modelled as an integrator. The length of side branch is limited between L_{min} and L_{max} , so there is some non-linear behaviour at these extremes. The value of $\langle p^2 \rangle$ is then used to adjust the overall exhaust stack transfer function

. It is important to note the the error is the mean squared pressure, and as such does not have a phase component.

Gradient descent controller

The pressure at the mouth of the exhaust stack is a function of frequency and the length of the side tubed. The pressure varies with both of these parameters in a nonlinear fashion. It is not possible to formulate the control problem in the classical sense, as the control signal, (the length of side tube), is not related to the error by a single complex gain. A gradient descent controller is proposed in which the length of the side tube is a function of the mean square pressure and the gradient of the mean square pressure with respect to the change in length.

As with all gradient descent algorithms where a closed form expression for the gradient is not readily available the step size of the algorithm has to be manually adjusted to find the optimal value, (optimal in the sense of minimising convergence time, overshoot and steady state error).

RESPONSE TO TEST SIGNALS

Three test cases are used to evaluate the controller.

Step change in frequency. The frequency of the source signal is changed by 10% and the convergence and steady state error is evaluated.

Chirp input. The source frequency is varied by 10% over 20 seconds and the error is evaluated

Sinusoidal change in frequency. The frequency varies by 10% in a sinusoidal manner over 20 seconds.

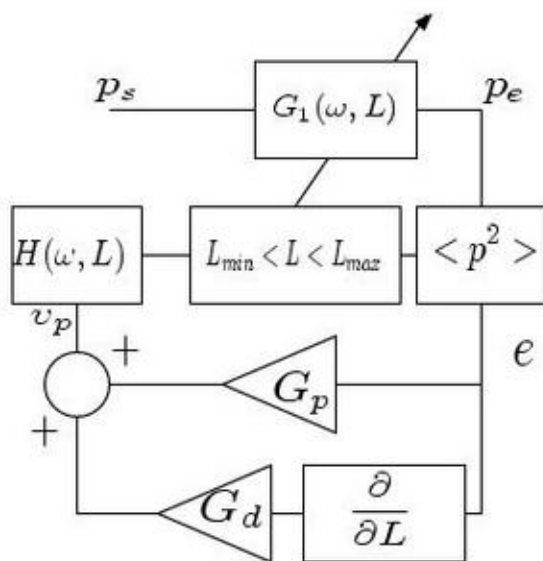


Figure 4 General controller diagram

GRADIENT DESCENT CONTROLLER.

Step Change

Figure (5) shows the pressure time history and the variation in the length of the side branch when the gradient descent controller is used. At 7.7 seconds the frequency of the drive signal changes from 200 to 180Hz (-10%). The step size was set to 0.0125m and the fill rate, (integrator gain) was set to 1mm/sec. The controller acted at a rate of 8Hz. So that 0.125seconds of pressure data was used to evaluate the mean pressure squared, this is approximately 22 cycles.

Figure (6) shows the error in dB relative to the initial value of the mean squared pressure. It can be seen that without control the error increases by 30dB at the step change in frequency. With the controller operating the error still increases momentarily but within 8 seconds is reduced to the initial level. The controller then reduces the level further by 5dB. It should be noted that the controller calculates the gradient offline, so that the variations in level due to this process are not shown in the pressure time history.

Chirp

Figure (9) and Figure (10) show the results for the chirp input. The chirp rate was set so that the fill rate could match the required change in length to maintain the minimum pressure radiation condition. It can be seen that as the pressure reduces due to the change in frequency, the length of the pipe does not change, however, once the pressure increases again the length of the pipe changes linearly with the change in drive frequency. The error is not reduced to its initial value, but it remains approximately 8dB less than the uncontrolled level.

Sinusoidal frequency change

Figure(13) and Figure(14) show the results for the chirp input. The chirp rate was set so that the fill rate could not match the required change in length to maintain the minimum pressure radiation condition. In this case the gradient descent controller, becomes unstable. Reduction of the gain only reduced the performance, and at no point did the controller manage to track the disturbance and minimise the level.

A HEURISTIC CONTROLLER

A simple heuristic or rule based controller is proposed. The length of the side branch is governed by the following rules

if new error > old error $\Delta L = -\Delta L$

new L = old L + ΔL

The controller always adds to the branch length, unless the error increases, in this case it decreases the length. The length is still limited between L_{min} and L_{max} . The pump also still acts as an integrator so that the pump rate determines how quickly the length can change.

In this algorithm, the size of the length change is used to change the performance. Too large a value will cause the level to change far too rapidly, and the controller will fluctuate about the optimal point. This can be mitigated by a low pump rate, which will slow the response of the whole system. Too small a value will cause the system to take a long time to adapt to changes in source frequency.

Step Change

Figure(7) shows the pressure time history and the variation in the length of the side branch when the rule based controller is used. At the frequency of the drive signal changes from 200 to 180Hz (-10%). The step size was set to 0.0125m and the fill rate, (integrator gain) was set to 1mm/sec. The controller acted at a rate of 8Hz. So that 0.125 seconds of pressure data was used to evaluate the mean pressure squared, this is approximately 22 cycles.

Figure(8) shows the error in dB relative to the initial value of the mean squared pressure. It can be seen that without control the error, it is a similar convergence as the gradient descent algorithm. However, it should be noted that this controller is working in real time, that is no off line calculation of

gradients has taken place. The error converges to the initial value by 7.7 seconds. However, the error is not reduced to less than the initial value, as was the case with the gradient descent controller.

Chirp

Figure (11) and Figure(12) show the results for the chirp input. The chirp rate was set so that the fill rate could match the required change in length to maintain the minimum pressure radiation condition. It can be seen that there is more variation in the level than there was in results for the gradient controller. It can also be seen that the changes in length are stepped, not smooth. The average level is higher than that achieved by the gradient descent controller.

Sinusoidal frequency change

Figure(15) and Figure(16) show the results for the rule based controller as the input frequency varies sinusoidally. In this test case the rule based controller performs better than the gradient descent based controller. The controller does not increase the level and the pressure is reduced by between 5 and 35dB. The variation in the side branch length can be seen to be approximately sinusoidal for part of the time history. This trend stops when the side branch length becomes zero. At this point the limiters in the controller algorithm prevent further reductions in length as a negative length is non-physical.

CONTROL PARAMETERS

The pump rate and the change in length at each control step, need to be matched to obtain the best performance from either controller. In applications the pump rate is likely to be limited to a small range, most likely at low values for low cost systems. This will reduce the agility of the control system. However the source frequency is not expected to change rapidly and as community annoyance levels are measured over a period of hours a few minutes of adaption time will not cause an issue.

CONCLUSIONS

This paper has presented a brief investigation into a adaptive side branch for an exhaust stack. It has been shown that a simple controller can be used to maintain a minimum amount of sound radiation. The rule based controller out performed the gradient descent controller when the frequency changed in a non linear fashion. Also the rule based controller does not required the calculation of a gradient and as such is simpler and faster.

Figure 5 (a) Pressure radiated from top of stack with and without gradient descent controller as the frequency steps from 200 to 180Hz. (b) Desired length and actual length of side branch as controller adapts.

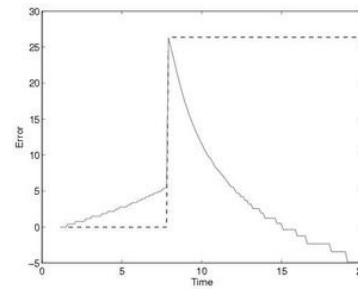


Figure 6 Error signal with and without gradient based controller as the frequency steps from 200 to 180Hz.

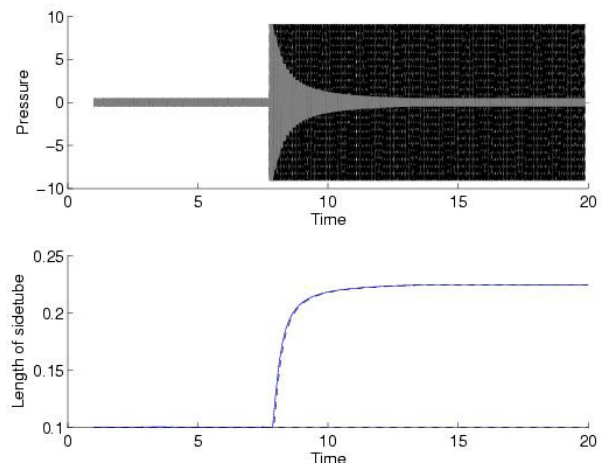


Figure 7 Pressure radiated from top of stack with and without rule based controller as the frequency steps from 200 to 180Hz. (b) Desired length and actual length of side branch as controller adapts.

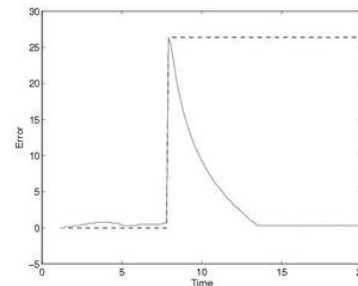


Figure 8 Error signal with and without rule based controller as the frequency steps from 200 to 180Hz.

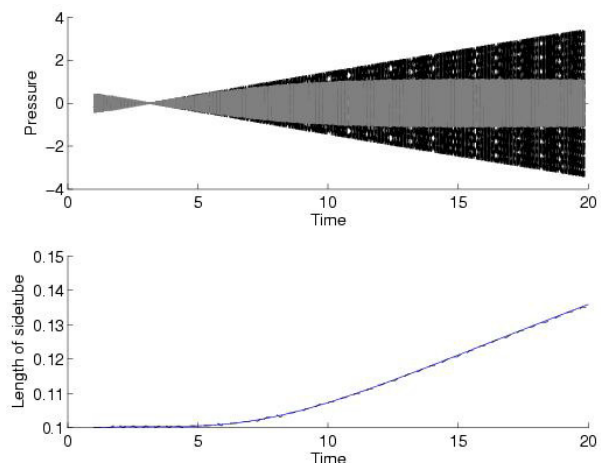
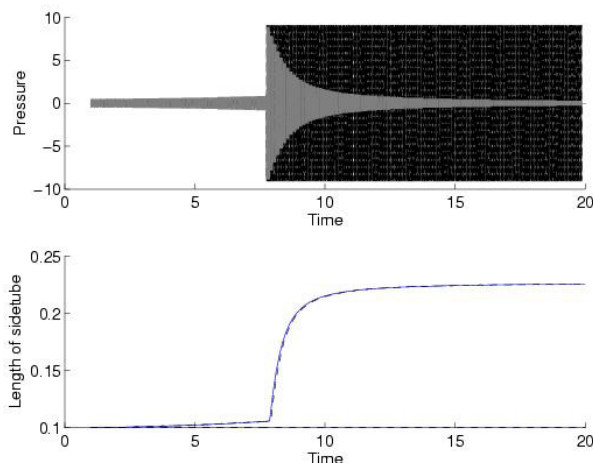


Figure 9 Pressure radiated from top of stack with and without gradient controller as the frequency linearly changes from 200 to 160Hz. (b) Desired length and actual length of side branch as controller adapts.

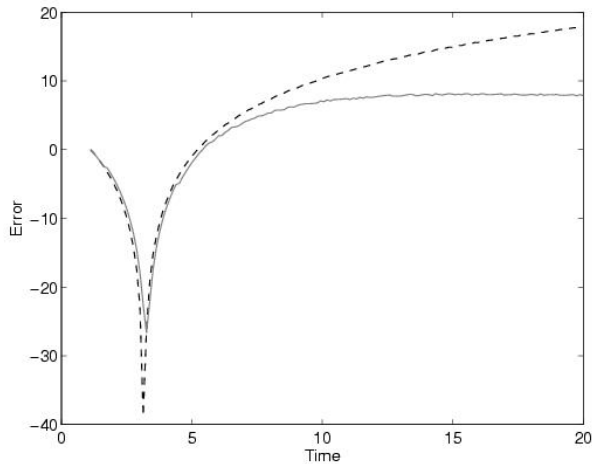


Figure 10 Error signal with and without gradient controller as the frequency linearly changes from 200 to 160Hz.

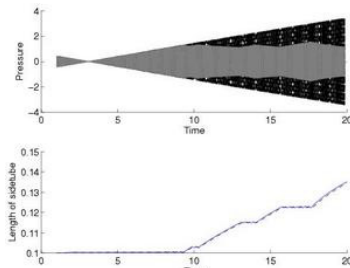


Figure 11 Pressure radiated from top of stack with and without rule based controller as the frequency linearly changes from 200 to 160Hz. (b) Desired length and actual length of side branch as controller adapts.

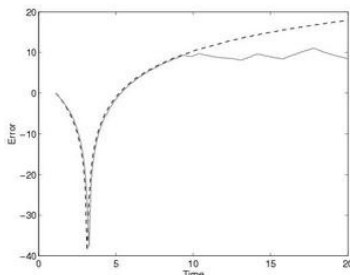


Figure 12 Error signal with and without rule based controller as the frequency linearly changes from 200 to 160Hz.

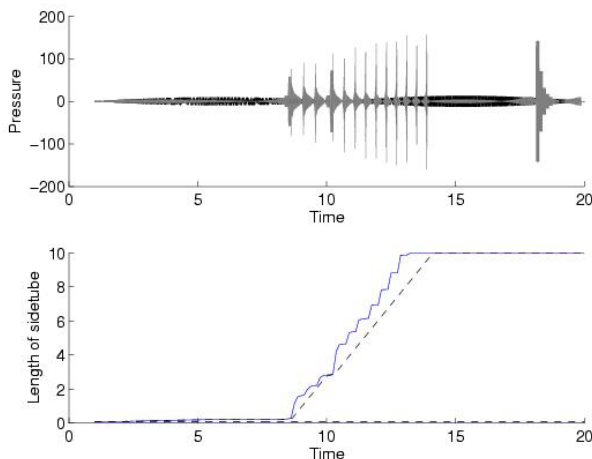


Figure 13 (a) Pressure radiated from top of stack with and without rule based controller as the frequency sinusoidally changes from 200 20Hz. (b) Desired length and actual length of side branch as controller adapts.

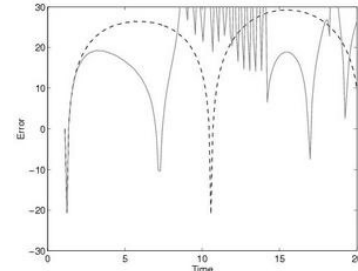


Figure 14 Error signal with and without gradient descent controller as the frequency sinusoidal changes from 200Hz 20Hz.

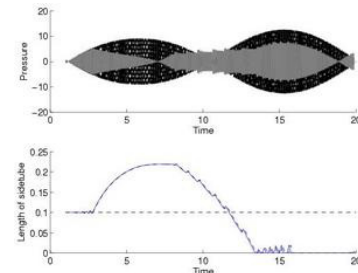


Figure 15 Pressure radiated from top of stack with and without rule based controller as the frequency sinusoidally changes from 200 20Hz. (b) Desired length and actual length of side branch as controller adapts.

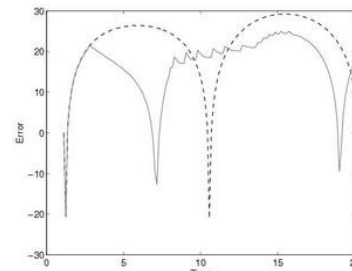


Figure 16 Error signal with and without rule based controller as the frequency sinusoidal changes from 200Hz 20Hz.

REFERENCES

(Bies 1992) Bies, D., & Hansen, C., Engineering Noise Control Theory and Practice, Second Edition, E & FN Spon, London, 1996.

(Beranek 1992) Beranek, L., & Ver, I., (Editors), Noise and Vibration Control Engineering Principles and Applications, Wiley Interscience, New York, 1992.

(Davies 2004) P. O. A. L. Davies K. R. Holland, The measurement and prediction of sound waves of arbitrary amplitude in practical flow ducts, Journal of Sound and Vibration Volume 271, Issues 3-5 , 6 April 2004, Pages 849-861

(Kinsler 1999) Kinsler, L., Frey, A., Coppens, A., & Sanders, J., Fundamentals of Acoustics, Wiley, New York, 1999

(Kostek 2000) Theodore M. Kostek, Matthew A. Francheck, Hybrid Noise Control In Ducts Journal of Sound and Vibration Volume 237, Issue 1 , 12 October 2000, Pages 81-100

(Selamet 1996) A. Selamet P. M. Radavich,, Side branches in automotive intake systems as noise generators. The Journal of the Acoustical Society of America -- April 1996 -- Volume 99, Issue 4, pp. 2460-2500